中国光学 Chinese Optics 核心期刊

兼具反射和透射模式的共振波导光栅滤波器的设计

樊丽娜 马军山

Design of resonant waveguide grating filter with reflection and transmission modes

FAN Li-na, MA Jun-shan

引用本文:
樊丽娜, 马军山. 兼具反射和透射模式的共振波导光栅滤波器的设计[J]. 中国光学, 2020, 13(5): 1147-1157. doi: 10.37188/CO.2020-0072
FAN Li-na, MA Jun-shan. Design of resonant waveguide grating filter with reflection and transmission modes[J]. *Chinese Optics*, 2020, 13(5): 1147-1157. doi: 10.37188/CO.2020-0072

在线阅读 View online: https://doi.org/10.37188/CO.2020-0072

文章编号 2095-1531(2020)05-1147-11

Design of resonant waveguide grating filter with reflection and transmission modes

FAN Li-na[1,2], MA Jun-shan[1*]
(1. *School of Optics-Electrical and Computer Engineering*, *University of Shanghai for Science and Technology*, *Shanghai* 200093, *China*;
2. *School of Mathematics and Physics*, *Suzhou University of Science and Technology*, *Suzhou* 215009, *China*)
* *Corresponding author*, *E-mail*: *junshanma@163.com*

Abstract: At present, narrow-band filter based on resonant waveguide grating structure applied to biosensors can only achieve a single filter mode of reflection or transmission. In order to expand the variety of samples and improve the accuracy of the samples testing, a resonant waveguide grating filter with both reflection and transmission modes was designed based on the guided mode resonance effect. Firstly, based on the classical one-dimensional resonant waveguide grating structure, a filter with convertible reflection-transmission mode at the same wavelength (632.8 nm) was designed by adjusting the incident conditions. In both modes, excellent filtering performance was presented, spectral efficiency was higher than 98%, and *Q* factor was greater than 1 000. Then, the resonance mechanism for that the same device can realize two filtering modes was analyzed. The results showed that the reflection and transmission narrow-band filtering modes could be converted at the designed wavelength with the same resonant waveguide grating structure under different incident conditions.

Key words: resonant waveguide grating; guided mode resonance; reflection mode; transmission mode; classical incidence; full conical incidence

兼具反射和透射模式的共振波导光栅滤波器的设计

樊丽娜[1,2], 马军山[1*]
(1. 上海理工大学 光电信息与计算机工程学院, 上海 200093;
2. 苏州科技大学 数理学院, 江苏 苏州 215009)

摘要: 目前, 应用于生物传感系统的共振波导光栅窄带滤波器仅能实现反射或透射的单一滤波模式。为了扩展被检样品

收稿日期: 2020-04-23; **修订日期:** 2020-05-13
基金项目: 国家自然科学基金项目(No.61775140)
Supported by National Natural Science Foundation of China (No.61775140)

的种类和提高样品的检测准确度，本文基于导模共振效应设计了兼具反射和透射模式的共振波导光栅滤波器。首先，基于经典的一维共振波导光栅结构，通过调节入射条件，设计了在同一波长（632.8 nm）处反射-透射模式可转换的滤波器，该滤波器在两种模式下均具有优良的滤波性能，光谱效率高于 98%，Q 因子大于 1 000。然后，从物理机制层面出发，分析了同一器件实现两种滤波模式的共振机理。结果表明：不同入射条件下，同一共振波导光栅结构在设计波长处可实现反射-透射窄带滤波模式的转换。

关　键　词：共振波导光栅；导模共振；反射模式；透射模式；经典入射；全圆锥入射

中图分类号：O436.1; TN25　　**文献标志码：**A　　**doi：**10.37188/CO.2020-0072

1 Introduction

Resonant waveguide grating is composed of a waveguide and a dielectric grating. Due to the interaction between the two components, the outgoing spectrum shows many unique optical characteristics when the light is incident on the device. This has become an important branch of label-free bio-sensing field[1-4]. In the biosensor system, resonant waveguide grating is used as narrow-band filter to usually check the samples by observing the narrow-band spectral drift before and after the sample attaching. In the early days, the researchers designed the narrow-band filters in reflection or transmission mode under classical incidence. Based on the resonant waveguide grating structure, they designed and developed the reflection filters that worked in different wavebands[5-7]. In the design, the period and fill factor of sub-wavelength grating, as well as the thickness and refractive index of grating and waveguide layer were adjusted to realize the reflection filtering function at a certain wavelength. In addition, a transmission filter was realized based on a more complex resonant waveguide grating structure that combined the multilayer high-reflection film structure with waveguide grating or adopted a grating in strong modulation[8-10].

The filters with the above two modes were both designed by changing the structural parameters of resonant waveguide gratings. In fact, as the resonant waveguide grating contains a periodic sub-wavelength grating layer, the spectral performance of the device is also strongly affected by the incident azimuth. Therefore, in recent years, the design of resonant waveguide grating devices under conical incident condition has become a research hotspot. The studies in this field mostly focus on the design of reflection filters, such as polarization-independent reflection filters[11-12] and tunable reflection filters[13-14]. The research group has developed the transmission filter of one-dimensional resonant waveguide grating under full conical incidence[15]. All the above resonant waveguide grating filters can only achieve a single reflection or transmission filtering function, so that when applied in the field of biosensors, they can only reflect or transmit light in the samples for sensing measurement. If a same filter device has both reflection and transmission filtering functions, its detection range will be greatly expanded, so that it can measure both the reflection and transmission properties of the sample. Therefore, in this paper, the classical and full-conical incident conditions will be combined to analyze the guided-mode resonance mechanism of a classical one-dimensional single-layer resonant waveguide grating. Taking the wavelength of 632.8 nm as an example, a narrow-band filter that can realize the conversion between reflection and transmission modes at the same wavelength has been developed, so as to expand the application scenarios of resonant waveguide grating filter and further promote its application in the bio-sensing field.

2 Design of a reflection-transmission convertible filter

2.1 Structure and design approach

Due to its simple structure and easy prepara-

tion, one-dimensional resonant waveguide grating is most commonly used to design narrow-band filter. Therefore, this classical structure model is adopted in this paper to analyze the resonance mechanism and design the reflection-transmission convertible filters. In order to obtain the narrow-band filter with the working wavelength of 632.8nm, the design is mainly carried out in two steps. At first, a transmission filter with good performance is obtained by optimizing the structural parameters and incident conditions. This is because, compared with reflection filtering, the transmission filtering of a resonant waveguide grating is relatively difficult to realize unless the incident angle is large within a certain range[15]. And then, based on the structural parameters, the reflection filtering is realized by changing the incident conditions (azimuth and incident angle).

As shown in Fig. 1, the one-dimensional single-layer resonant waveguide grating consists of a substrate and a grating layer. Based on the above design method, the optimized structural parameters are as follows: the refractive indices of the grating ridge and slot in the rectangular grating layer are n_H = 1.72 and n_L = 1.50 respectively, the thickness of grating layer is d = 179 nm, the grating period is Λ = 564 nm, and the fill factor is f = 0.6. In this structure, the grating layer also acts as the waveguide layer. According to the equivalent medium theory[16], its equivalent refractive index for Transverse Electric (TE) polarized light is approximately $n_{eff} = \sqrt{n_H^2 f + n_L^2 (1-f)} = 1.636$. The refractive indices of the covering layer and substrate are n_c = 1.0 and n_s = 1.50 respectively. The TE polarized light is obliquely incident from the top of the device. The azimuth and incident angle of incident light are denoted by φ and θ respectively. The azimuth φ is the included angle between the incident plane and the grating vector (in x-axis in Fig. 1). The incident angle θ is the included angle between the incident light and the normal line of the incident plane.

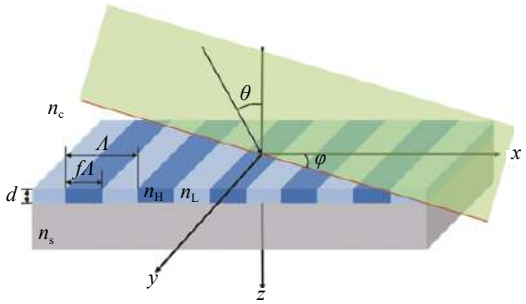

Fig. 1　Structural diagram of single-layer resonant waveguide grating (Structure parameters: n_H = 1.72, n_L = 1.50, d = 179 nm, Λ = 564 nm, f = 0.6, n_c = 1.0, n_s = 1.50)

图 1　单层共振波导光栅结构示意图（结构参数：n_H = 1.72, n_L = 1.50, d = 179 nm, Λ = 564 nm, f = 0.6, n_c = 1.0, n_s = 1.50）

2.2　Calculation results and discussion

The transmission spectral characteristics of the structure designed in Fig. 1 can be calculated by using Rigorous Coupled-Wave Analysis (RCWA)[17−19]. In order to achieve the reflection filtering function at a single wavelength of 632.8 nm and ensure no other resonance within the spectral range of ±100 nm, the adjustable range of incident angle is defined as 20º~25º under classical incidence (ϕ = 0º). As shown in Fig. 2(a), as the incident angle increases, the resonance wavelength will decrease gradually, and the transmittance at the resonance wavelength will stay at an extremely low level. When the incident angle is large, the transmission filtering function can be realized under full conical incidence (ϕ = 90º)[15]. Therefore, the structural parameters as shown in Fig. 1 are still adopted and the incident condition is changed into full conical incidence (ϕ = 90º). As shown in Fig. 2(b), when the incident angle between 80º~89º increases, the resonance peak will drift to the short-wave direction, and the sideband transmittance will gradually decrease. However, when the incident angle is close to 90º, the transmittance of resonance peak will decrease due to the weakening of the coupling between evanescent higher-order diffraction wave and guided mode. As

shown in Fig. 2(b), when the incident angle is less than 88º, the peak transmittance is greater than 95%.

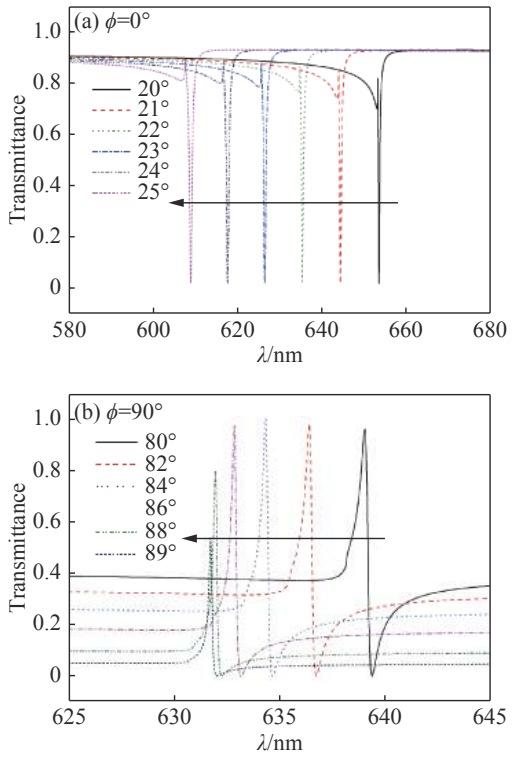

Fig. 2 Transmission spectra for different incident angles (a) classical incidence; (b) full conical incidence

图 2 不同入射角下的透射光谱图（a)经典入射; (b)全圆锥入射

The above analysis results show that, for resonant waveguide grating devices with the same structural parameters, it is possible to realize the conversion between reflection and transmission filtering modes by adjusting the incident conditions. Under the two incident conditions, the resonance wavelength can be changed by adjusting the incident angle. To realize the conversion between reflection and transmission filtering modes at the same wavelength (632.8 nm), the relationship between resonance wavelength and incident angle under the two incident conditions has been further analyzed. The analysis results are shown in Fig. 3. As shown in Fig. 3(a), under classical incidence, the resonance wavelength will decrease almost linearly as the incident angle increases. When the incident angle is 22.28º, the resonance wavelength is 632.8 nm. As shown in Fig. 3(b), under full conical incidence, the resonance wavelength will gradually decrease as the incident angle increases. When the incident angle is 86.08º, the resonance wavelength is 632.8 nm. Thus, when the incident angles under classical and full conical incident conditions are 22.28º and 86.08º respectively, the resonant waveguide grating device has both reflection and transmission narrow-band filtering functions at the wavelength of 632.8 nm.

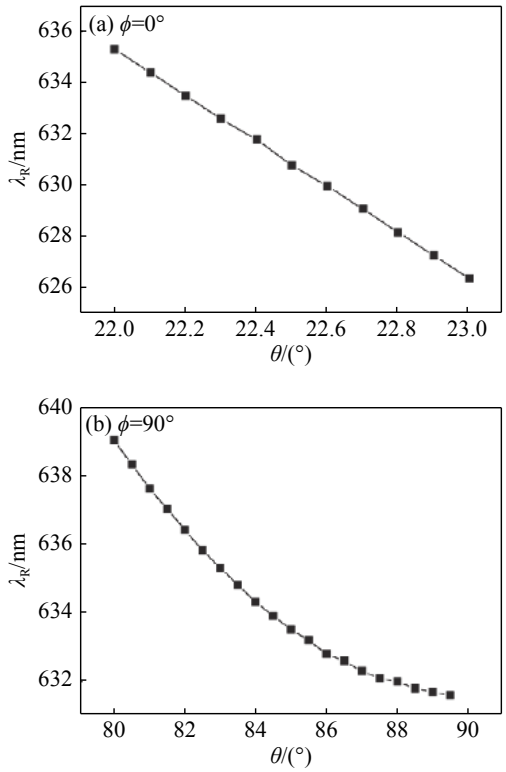

Fig. 3 Relationship between resonance wavelength and incident angle. (a) Classical incidence; (b) full conical incidence

图 3 共振波长随入射角变化图。(a)经典入射; (b)全圆锥入射

The 0th-order transmission spectra of the reflection-transmission convertible narrow-band filter is shown in Fig. 4. It can be seen that the spectral characteristics under classical and full conical incident conditions are opposite. Under classical incidence, the designed resonant waveguide grating structure is characterized by reflection filtering, and

the wavelength corresponding to transmission valley is 632.8nm. At this wavelength, the transmittance is only 1.9%, the linewidth is 0.58 nm, and the Q factor is 1 090. Under the condition of full conical incidence, the same structure is characterized by transmission filtering, with a peak wavelength of 632.8nm, a peak transmittance of 98%, a linewidth of 0.35 nm and a Q factor of 1 808. The designed filter has excellent spectral performance in both reflection and transmission filtering modes.

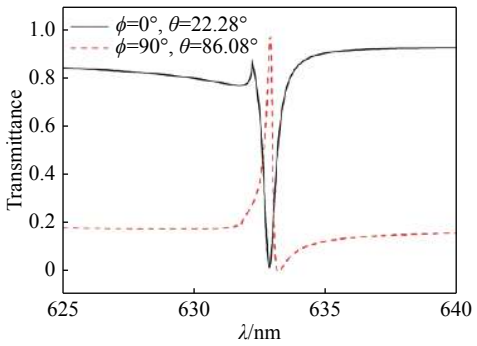

Fig. 4　Transmission spectra under different incident conditions

图 4　不同入射条件下的透射光谱图

2.3　Analysis of resonance mechanism

Based on the principle of guided mode resonance, we used the MATLAB to analyze the resonance mechanism of the above reflection-transmission convertible filter under different incident conditions. According to the phase matching condition, we obtained[13]:

$$\beta_m = k_0\sqrt{n_c^2\sin^2\theta + 2n_c\sin\theta\cos\varphi i\frac{\lambda}{\Lambda} + i^2\frac{\lambda^2}{\Lambda^2}}, \quad (1)$$

where β_m is the propagation constant of the m-th guided mode; $k_0 = 2\pi / \lambda$; λ is the wavelength of incident light; and i is the diffraction order. For classical incidence, the Eq. (1) can be simplified as:

$$\begin{aligned}\beta_m &= k_0\sqrt{n_c^2\sin^2\theta + 2n_c\sin\theta\, i\frac{\lambda}{\Lambda} + i^2\frac{\lambda^2}{\Lambda^2}}\\ &= k_0\left(n_c\sin\theta + i\frac{\lambda}{\Lambda}\right).\end{aligned} \quad (2)$$

For full conical incidence, the Eq. (1) can be simplified as:

$$\beta_m = k_0\sqrt{n_c^2\sin^2\theta + i^2\frac{\lambda^2}{\Lambda^2}}. \quad (3)$$

According to the Eq. (3), the guided modes excited by ±ith-order diffraction waves under the condition of full conical incidence are degenerate.

Then it is combined with the eigenvalue equation of single-layer waveguide grating[20]:

$$\tan(k_m d) = \frac{k_m(\gamma_m + \delta_m)}{k_m^2 - \gamma_m\delta_m},\ \text{TE} \quad (4)$$

$$\tan(k_m d) = \frac{n_{eff}^2 k_m(n_s^2\gamma_m + n_c^2\delta_m)}{n_s^2 n_c^2 k_m^2 - n_{eff}^4\gamma_m\delta_m},\ \text{TM} \quad (5)$$

where $\gamma_m = (\beta_m^2 - k_0^2 n_s^2)^{1/2}$, $k_m = (k_0^2 n_{eff}^2 - \beta_m^2)^{1/2}$ and $\delta_m = (\beta_m^2 - k_0^2 n_c^2)^{1/2}$ are the wave numbers along the z-axis direction in the cover layer, grating layer and substrate respectively. Under classical incidence, TE polarized-light incidence can only excite the TE guided mode in the waveguide layer. The curves in Fig. 5(a) are the positions where the +1st-order and −1st-order diffraction waves resonate with the TE_0 guided mode, as estimated according to Eq. (3) and Eq. (4), and are expressed as $TE_{+1,0}$ and $TE_{-1,0}$ respectively. For the designed single-layer resonant waveguide grating structure $d/\Lambda = 179/564 = 0.3174$ (expressed as dotted line), the intersections of the dotted line and curves are the positions where the filter structure resonates under classical incidence. It can be seen from Fig. 5(a) that the dotted line only intersects the $TE_{+1,0}$ curve and that the point of intersection corresponds to the narrow-band reflection filtering wavelength of 632.8 nm. This indicates that, under this incident condition, only the resonance between +1st-order diffraction wave and TE_0 guided mode will occur in the designed structure. Different from classical incidence, the full conical incidence of TE polarized light can excite the TE_0 and TM_0 guided modes[11]. Under the condition of full conical incidence, the guided modes excited by ±ith-order diffraction waves are degenerate,

namely, $TE_{+1,0}$ and $TE_{-1,0}$ are degenerate into $TE_{1,0}$, and $TM_{+1,0}$ and $TM_{-1,0}$ are degenerate into $TM_{1,0}$. The curves in Fig. 5(b) are the positions where the diffraction waves resonate with the TE_0 and TM_0 guided modes, as estimated according to Eq. (3), Eq. (4) and Eq. (5). Similarly, the intersections of the dotted line and curves are the resonance positions of the designed filter structure. As seen from Fig. 5(b), the dotted line only intersects the $TE_{1,0}$ curve and the point of intersection corresponds to the narrow-band transmission filtering wavelength of 632.8 nm. This indicates that, under this incident condition, the designed structure has only one resonance peak, which is caused by the resonance between ±1st-order diffraction waves and TE_0 guided mode.

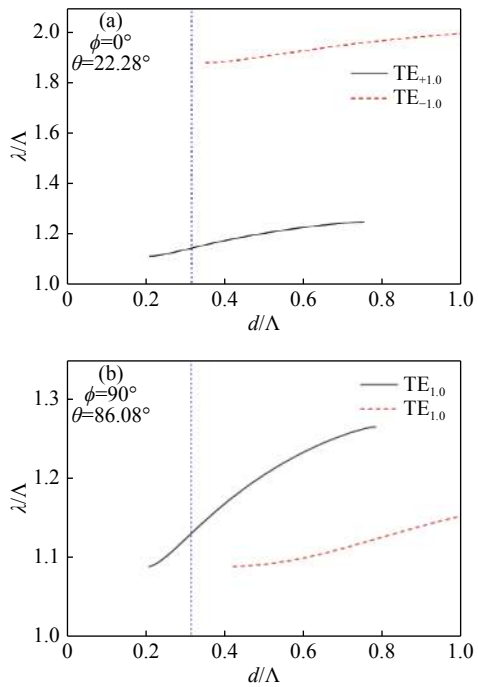

Fig. 5 Resonance locations estimated based on phase matching condition and eigenvalue equation. (a) Azimuth: 0º, incident angle: 22.28º; (b) azimuth: 90º, incident angle: 86.08º

图 5 基于相位匹配条件和本征方程估算的共振位置。(a)方位角 0º, 入射角 22.28º; (b)方位角 90º, 入射角 86.08

The Fig. 6 (color online) shows the electric field spatial distribution of a one-cycle resonant waveguide grating structure in the *x*-*z* plane. As shown in the figure, under classical and full conical incident conditions, the evanescent higher-order diffraction wave is coupled with the TE_0 guided mode due to phase matching, so the resonance behavior occurs at the wavelength of 632.8 nm. Under the two incident conditions, local electric field enhancement is observed in the grating-waveguide layer, and the enhanced electric field gradually penetrates the substrate. The difference under the two conditions is that the electric field penetrates the substrate more strongly under full conical incidence. This indicates that the coupling between diffraction wave and guided mode in the resonant waveguide grating structure under full conical incidence is weaker than that under classical incidence, resulting in a narrower linewidth in the transmission filtering mode (as shown in Fig. 4).

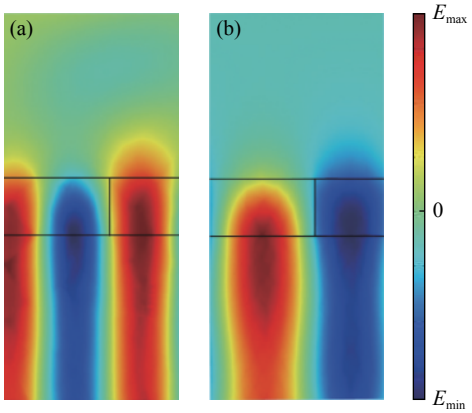

Fig. 6 Spatial distribution of electric field at the resonance wavelength of 632.8 nm. (a) Azimuth: 0º, incident angle: 22.28º; (b) Azimuth: 90º, incident angle: 86.08º

图 6 共振波长 632.8 nm 处电场空间分布图。(a)方位角 0º, 入射角 22.28º; (b)方位角 90º, 入射角 86.08º

3 Conclusion

In this paper, based on the theory of guided mode resonance, a theoretical design method for one-dimensional single-layer resonant waveguide grating to realize the reflection-transmission convertible narrow-band filtering is presented. In the

case of TE polarized-light incidence, the same device can realize the conversion between reflection and transmission filtering modes by adjusting the azimuth and incident angle. Under classical incidence, reflection filtering mode is observed when the incident angle is 22.28º, and the reflection filtering at the resonance wavelength of 632.8 nm is caused by the resonance between +1st-order diffraction wave and TE_0 guided mode. Under full conical incidence, transmission filtering mode is observed when the incident angle is 86.08º, and the transmission filtering at the resonance wavelength of 632.8 nm is caused by the resonance between ±1st-order diffraction waves and TE_0 guided mode. This method can also be applied to the design of reflection-transmission convertible filter based on one-dimensional multilayer resonant waveguide grating structure, and can be extended to any specified working wavelength by adjusting the structural parameters such as grating layer thickness and period. As this design method makes two filtering modes available for the same device, its use is expected to expand the varieties of tested samples and improve the detection accuracy of the samples in the bio-sensing measurement.

——中文对照版——

1　引　言

共振波导光栅由波导与介质光栅组成，由于二者的相互作用，当入射光照射在器件上时，出射光谱呈现许多奇特的光学特性，现已成为免标记生物传感领域[1-4]的一个重要分支。在生物传感系统中，共振波导光栅被用作窄带滤波器，常通过观测样品附着前后窄带光谱的漂移来实现对样品的检测。早期，研究人员都是以经典入射条件为前提设计反射模式或透射模式的窄带滤波器。基于共振波导光栅结构，研究人员设计开发了工作于不同波段的反射滤波器[5-7]，设计中常通过调节亚波长光栅的周期、占空比、光栅及波导层的厚度和折射率等参数来实现某一波长的反射滤波功能。此外，采用较复杂的共振波导光栅结构，诸如将多层高反膜结构与波导光栅相结合、强调制光栅等方法，实现了共振波导光栅透射滤波器[8-10]。

以上两种模式滤波器的设计均是通过改变共振波导光栅的结构参数来实现的。其实，由于共振波导光栅含有周期性的亚波长光栅层，器件的光谱性能还强烈地受到入射方位角的影响。为此，近年来采用圆锥入射条件设计共振波导光栅器件成为研究热点，这方面的研究大多集中于反射滤波器的设计，诸如偏振无关的反射滤波器[11-12]、可调反射滤波器[13-14]等。课题组已在全圆锥入射条件下实现了一维共振波导光栅的透射滤波器[15]。然而以上各种形式的共振波导光栅滤波器都仅能实现单一的反射或透射滤波功能，使得其在生物传感领域应用时，仅能对样品进行反射或透射的传感测量。如果同一器件能够兼具反射和透射滤波模式，将极大地扩展滤波器的检测范围，使得其既能测量样品的反射信息又能测量透射信息。为此，本文将结合经典入射和全圆锥入射条件，分析经典的一维单层共振波导光栅的导模共振机理，以 632.8 nm 波长为例，实现同一器件在同一波长处反射-透射模式可转换的窄带滤波，从而拓展共振波导光栅滤波器的应用场景，进一步推动其在生物传感领域的应用。

2　反射-透射模式可转化滤波器设计

2.1　结构与设计方法

由于结构简单、易于制备，一维共振波导光栅最常用于设计窄带滤波器，因此，本文采用这一经典结构模型进行共振机理分析和反射-透射可转换滤波器设计。为了获得工作波长为 632.8 nm 的窄带滤波器，本设计主要分两步进行。首先，通

过结构参数和入射条件的优化获得性能优良的透射式的滤波器。因为，相较于反射滤波模式，共振波导光栅的透射滤波模式相对较难实现，它需要在一定的大入射角范围内才可实现[15]。然后，在此结构参数的基础上，通过改变入射条件（方位角和入射角）来实现反射滤波模式。

图 1 所示一维单层共振波导光栅由基底和光栅层组成。基于上述设计方法，优化后的结构参数如下：矩形光栅层中栅脊和栅槽的折射率分别为 $n_H = 1.72$, $n_L = 1.50$, 光栅层厚度为 $d = 179$ nm, 光栅周期为 $\Lambda = 564$ nm, 填充因子为 $f = 0.6$。在此结构中光栅层同时也作为波导层，根据等效介质理论[16]，其对于横电 (TE) 偏振光的等效折射率约为 $n_{eff} = \sqrt{n_H^2 f + n_L^2 (1-f)} = 1.636$。覆盖层和基底折射率分别为 $n_c = 1.0$, $n_s = 1.50$。TE 偏振光从器件顶部斜入射，入射光的方位角和入射角分别用 φ 和 θ 表示。其中，方位角 φ 为入射平面与光栅矢量（沿图 1 中 x 轴方向）之间的夹角，入射角 θ 为入射光与入射表面法线之间的夹角。

2.2 计算结果与讨论

利用严格耦合波理论 (RCWA)[17-19] 可计算图 1 所示结构的透射光谱特性。在经典入射 ($\varphi = 0°$) 条件下，为了确保在单一波长 632.8 nm 处实现反射滤波性能且在±100 nm 的光谱范围内无其它共振，设定入射角调节范围为 20°~25°。图 2 为经典入射和全圆锥入射的透射光谱图。由图 2(a) 可知，随着入射角增大，共振波长逐渐减小，且共振波长处维持极低的透射率。在全圆锥入射 ($\varphi = 90°$) 条件下，入射光以大角度入射时，可实现透射滤波功能[15]。仍然采用图 1 所示的结构参数，将入射条件改变为全圆锥入射 ($\varphi = 90°$)。由图 2(b) 可知，当入射角取值为 80°~89°时，随着入射角的增大，共振峰向短波方向漂移，同时旁带透射率逐渐减小。然而入射角接近 90°时，共振峰的透射率变低，这是由于接近 90°入射，倏逝的高级次衍射波与导模的耦合强度变弱。如图 2(b) 所示，当入射角小于 88°时，峰值透过率均大于 95%。

以上分析结果表明，对于同一结构参数的共振波导光栅器件，通过调节入射条件可能实现反射和透射滤波模式的转换。在两种入射条件下，调节入射角可导致共振波长的变化。为了实现同一波长（632.8 nm）处反射-透射滤波模式的转换，进一步分析了两种入射条件下共振波长随入射角的变化关系，结果如图 3 所示。由图 3(a) 可知，经典入射下，共振波长随入射角增大几乎线性地减小，当入射角为 22.28°时，共振波长为 632.8 nm。由图 3(b) 可知，全圆锥入射下，随着入射角增大，共振波长缓慢减小，当入射角为 86.08°时，共振波长为 632.8 nm。由此，可确定在经典入射和全圆锥入射两种情况下，入射角分别为 22.28°和 86.08°时，共振波导光栅器件在波长 632.8 nm 处兼具反射和透射窄带滤波功能。

图 4 为反射-透射可转换窄带滤波器的 0 级透射光谱图。可见，经典入射和全圆锥入射条件下呈现相反的光谱特征。经典入射下，设计的共振波导光栅结构呈现反射滤波特征，透射谷对应波长为 632.8 nm，此波长处透过率仅为 1.9%，线宽为 0.58 nm，Q 因子为 1090；而全圆锥入射下，同样的结构可呈现出透射滤波特征，峰值波长为 632.8 nm，峰值透过率为 98%，线宽为 0.35 nm，Q 因子为 1808。设计的滤波器在反射和透射滤波模式下均具有优良的光谱性能。

2.3 共振机理分析

基于导模共振原理，本文采用 MATLAB 软件分析了上述反射-透射可转换滤波器在不同入射条件下的共振机理。根据相位匹配条件[13]，有：

$$\beta_m = k_0 \sqrt{n_c^2 \sin^2\theta + 2n_c \sin\theta \cos\varphi i\frac{\lambda}{\Lambda} + i^2\frac{\lambda^2}{\Lambda^2}}, \quad (1)$$

其中 β_m 表示第 m 级导模的传播常数，$k_0 = 2\pi/\lambda$，λ 为入射光波长，i 表示衍射级。对于经典入射，公式 (1) 可简化为：

$$\begin{aligned}\beta_m &= k_0 \sqrt{n_c^2 \sin^2\theta + 2n_c \sin\theta\, i\frac{\lambda}{\Lambda} + i^2\frac{\lambda^2}{\Lambda^2}} \\ &= k_0\left(n_c \sin\theta + i\frac{\lambda}{\Lambda}\right),\end{aligned} \quad (2)$$

而对于全圆锥入射，公式 (1) 可简化为：

$$\beta_m = k_0 \sqrt{n_c^2 \sin^2\theta + i^2\frac{\lambda^2}{\Lambda^2}}. \quad (3)$$

由公式 (3) 可知，全圆锥入射条件下±i 级衍

射波激发的导模是简并的。

结合单层波导光栅的本征方程[20]:

$$\tan(k_m d) = \frac{k_m(\gamma_m + \delta_m)}{k_m^2 - \gamma_m \delta_m}, \text{ TE} \qquad (4)$$

$$\tan(k_m d) = \frac{n_{eff}^2 k_m (n_s^2 \gamma_m + n_c^2 \delta_m)}{n_s^2 n_c^2 k_m^2 - n_{eff}^4 \gamma_m \delta_m}, \text{ TM} \qquad (5)$$

其中 $\gamma_m = (\beta_m^2 - k_0^2 n_s^2)^{1/2}$, $k_m = (k_0^2 n_{eff}^2 - \beta_m^2)^{1/2}$, $\delta_m = (\beta_m^2 - k_0^2 n_c^2)^{1/2}$分别为覆盖层、光栅层和基底中沿 z 方向的波数。经典入射下, TE 偏振光入射仅能激发波导层中的 TE 导模, 图 5(a) 中曲线为根据公式 (3) 和公式 (4) 估算的+1 级和−1 级衍射波与 TE_0 导模发生共振的位置, 分别表示为 $TE_{+1,0}$ 和 $TE_{-1,0}$。对于设计的单层共振波导光栅结构 d/Λ = 179/564 = 0.3174(图中用点线表示), 点线与曲线的交点即为滤波器结构在经典入射下的共振位置。由图 5(a) 可知, 点线仅与 $TE_{+1,0}$ 曲线有交点, 此点对应的窄带反射滤波波长为 632.8 nm, 表明所设计结构在此入射条件下仅有+1 级衍射波与 TE_0 导模发生共振。不同于经典入射, 全圆锥入射条件下, TE 偏振光入射可以激发 TE_0 和 TM_0 导模[11]。全圆锥条件下, ±1 级衍射波激发的导模是简并的, 即 $TE_{+1,0}$ 和 $TE_{-1,0}$ 简并为 $TE_{1,0}$, $TM_{+1,0}$ 和 $TM_{-1,0}$ 简并为 $TM_{1,0}$。图 5(b) 中曲线为根据公式 (3) 和式 (4)、式 (5) 估算的衍射波与 TE_0 和 TM_0 导模发生共振的位置。同理, 点线与曲线的交点为所设计滤波器结构的共振位置。由图 5(b) 可知, 点线仅与 $TE_{1,0}$ 曲线有交点, 此点对应的窄带透射滤波波长为 632.8 nm。上述结果表明设计结构在此入射条件下仅有一个共振峰, 此峰是由于±1 级衍射波与 TE_0 导模的共振引起的。

图 6 为一个周期的共振波导光栅结构在 x-z 平面内的电场空间分布图。如图 6 所示, 在经典入射和全圆锥入射条件下, 在 632.8 nm 共振波长处, 由于倏逝的高级次衍射波与 TE_0 导模满足相位匹配条件而发生耦合, 发生共振。两种入射条件下光栅-波导层中均呈现局域的电场增强效应, 且增强的电场向基底方向渗透。所不同的是, 在全圆锥入射时, 电场向基底方向的渗透更强, 它表明此时共振波导光栅结构中衍射波与导模的耦合强度要低于经典入射时的情形, 导致透射滤波模式下具有更窄的线宽(如图 4 所示)。

3　结　论

本文基于导模共振理论建立了采用一维单层共振波导光栅实现反射-透射可转换窄带滤波器的理论设计方法, 指出了对于同一器件结构, 其反射和透射滤波模式均源于导模共振效应。TE 偏振光入射时, 通过调整方位角和入射角, 同一器件可实现反射-透射滤波模式的转换。经典入射条件下, 入射角为 22.28°时滤波器呈现反射滤波特征, 共振波长 632.8 nm 处的反射滤波模式是由+1 级衍射波与 TE_0 导模共振引起的; 全圆锥入射条件下, 入射角为 86.08°时滤波器呈现透射滤波特征, 共振波长 632.8 nm 处的透射滤波模式是由±1 级衍射波与 TE_0 导模共振引起的。此方法也可适用于一维多层共振波导光栅结构的反射-透射模式可转换滤波器的设计, 且通过调整光栅层厚度和周期等结构参数可拓展至任意指定工作波长。由于本设计方法使得一个器件具备了两种滤波模式, 在生物传感测量中有望用于扩展被检样品的种类和提高样品的检测准确度。

参考文献:

[1] CUNNINGHAM B, LIN B, QIU J, *et al*.. A plastic colorimetric resonant optical biosensor for multiparallel detection of label-free biochemical interactions[J]. *Sensors and Actuators B*: *Chemical*, 2002, 85(3): 219-228.

[2] JIA K H, ZHANG D W, MA J SH. Sensitivity of guided mode resonance filter-based biosensor in visible and near infrared ranges[J]. *Sensors and Actuators B*: *Chemical*, 2011, 156(1): 194-197.

[3] 齐攀, 李莹, 冯明创, 等. 用于阵列样品检测的扫描式表面等离子体共振生物传感器[J]. 光学 精密工程, 2012, 20(11): 2365-2372.
QI P, LI Y, FENG M CH, *et al*.. Scanning surface plasmon resonance biosensor for array sample detection[J]. *Optics*

and Precision Engineering, 2012, 20(11): 2365-2372. (in Chinese)

[4] 王弋嘉, 张崇磊, 王蓉, 等. 差分干涉表面等离子体共振传感器的优化与验证[J]. 光学 精密工程, 2013, 21(3): 672-679.
WANG Y J, ZHANG CH L, WANG R, *et al*.. Optimization and validation of differential interferometric surface plasmon resonance sensor[J]. *Optics and Precision Engineering*, 2013, 21(3): 672-679. (in Chinese)

[5] 麻健勇, 刘世杰, 魏朝阳, 等. 反射型导模共振滤波器设计[J]. 物理学报, 2008, 57(2): 827-832.
MA J Y, LIU SH J, WEI CH Y, *et al*.. Design of reflection resonant grating filters[J]. *Acta Physica Sinica*, 2008, 57(2): 827-832. (in Chinese)

[6] ZHONG Y, GOLDENFELD Z, LI K, *et al*.. Mid-wave infrared narrow bandwidth guided mode resonance notch filter[J]. *Optics Letters*, 2017, 42(2): 223-226.

[7] 刘振扬, 关宝璐, 胡丕丽, 等. 超窄线宽导模共振滤波器的设计[J]. 半导体光电, 2019, 40(1): 72-76.
LIU ZH Y, GUAN B L, HU P L, *et al*.. Design of resonant filter for ultra-narrow linewidth guide mode[J]. *Semiconductor Optoelectronics*, 2019, 40(1): 72-76. (in Chinese)

[8] SAKAT E, VINCENT G, GHENUCHE P, *et al*.. Guided mode resonance in subwavelength metallodielectric free-standing grating for bandpass filtering[J]. *Optics Letters*, 2011, 36(16): 3054-3056.

[9] 李业, 王琦, 王建宇, 等. 基于导模共振效应的宽带宽透射型滤波器的设计与优化[J]. 光子学报, 2016, 45(4): 0423002.
LI Y, WANG Q, WANG J Y, *et al*.. Design and optimization of wide-band filter based on guided mode resonant grating[J]. *Acta Photonica Sinica*, 2016, 45(4): 0423002. (in Chinese)

[10] FERRARO A, TANGA A A, ZOGRAFOPOULOS D C, *et al*.. Guided mode resonance flat-top bandpass filter for terahertz telecom applications[J]. *Optics Letters*, 2019, 44(17): 4239-4242.

[11] LACOUR D, GRANET G, PLUMEY J P, *et al*.. Polarization independence of a one-dimensional grating in conical mounting[J]. *Journal of the Optical Society of America A*, 2003, 20(8): 1546-1552.

[12] WANG W, CAI W, SHI ZH, *et al*.. Polarization-insensitive one-dimensional guided-mode resonance filter operating at conical mounting[J]. *Optics Letters*, 2018, 43(21): 5226-5229.

[13] YUKINO R, SAHOO P K, SHARMA J, *et al*.. Wide wavelength range tunable one-dimensional silicon nitride nano-grating guided mode resonance filter based on azimuthal rotation[J]. *AIP Advances*, 2017, 7(1): 015313.

[14] WANG W, GAO X M, SHEN X F, *et al*.. Spectral responses of linear grating filters under full-conical incidence[J]. *Optics Letters*, 2018, 43(3): 391-394.

[15] FAN L N, JIA K H, MA J SH. Transmission filter controlled by incident conditions in single-layer waveguide grating structures[J]. *Applied Optics*, 2019, 58(31): 8371-8375.

[16] BRUNDRETT D L, GLYTSIS E N, GAYLORD T K. Homogeneous layer models for high-spatial-frequency dielectric surface-relief gratings: conical diffraction and antireflection designs[J]. *Applied Optics*, 1994, 33(13): 2695-2706.

[17] MOHARAM M G, GAYLORD T K. Diffraction analysis of dielectric surface-relief gratings[J]. *Journal of the Optical Society of America*, 1982, 72(10): 1385-1392.

[18] 樊叔维. 二元光栅衍射特性的矢量理论分析[J]. 光学 精密工程, 1999, 7(5): 30-36.
FAN SH W. The vector theory analysis of binary gratings diffraction characteristics[J]. *Optics and Precision Engineering*, 1999, 7(5): 30-36. (in Chinese)

[19] 曹召良, 卢振武, 李凤友, 等. 二维抗反射亚波长周期结构光栅的设计分析[J]. 光学 精密工程, 2002, 10(6): 537-541.
CAO ZH L, LU ZH W, LI F Y, *et al*.. Design consideration of two-dimensional anti-reflective subwavelength periodic gratings[J]. *Optics and Precision Engineering*, 2002, 10(6): 537-541. (in Chinese)

[20] WANG S S, MAGNUSSON R. Theory and applications of guided-mode resonance filters[J]. *Applied Optics*, 1993, 32(14): 2606-2613.

Author Biographics:

Fan Lina (1980—), female, born in Yuci, Shanxi. She is a doctoral candidate and an experimentalist. She received her Bachelor's degree from Shanxi Normal University in 2002 and her master's degree from Suzhou University in 2005. She is mainly engaged in the research of micro-nano optical devices. E-mail: lnfan@mail.usts.edu.cn

樊丽娜(1980—),女,山西榆次人,博士研究生,实验师,2002 年于山西师范大学获得学士学位,2005 年于苏州大学获得硕士学位,主要从事微纳光学器件方面的研究。E-mail: lnfan@mail.usts.edu.cn

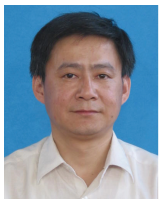

Ma Junshan (1967—), male, born in Harbin, Heilongjiang. He is a doctor, professor and doctoral supervisor. He received his doctorate in engineering from Harbin Institute of Technology in 1999. He is mainly engaged in the research of optical instruments and optical-communication photonic devices. E-mail: junshanma@163.com

马军山(1967—),男,黑龙江哈尔滨人,博士,教授,博士生导师,1999 年于哈尔滨工业大学获得工学博士学位,主要从事光学仪器、光通信光子器件方面的研究。E-mail: junshanma@163.com